SIAM J. NUMER. ANAL.
Vol. 52, No. 5, pp. 2440–2465

THE CONTROL OF PARASITISM IN G-SYMPLECTIC METHODS*

JOHN C. BUTCHER†, YOUSAF HABIB‡, ADRIAN T. HILL§, AND TERENCE J. T. NORTON§

Abstract. G-symplectic general linear methods are designed to approximately preserve symplectic invariants for Hamiltonian systems. In this paper, the properties of G-symplectic methods are explored computationally and theoretically. Good preservation properties are observed over long times for many parameter ranges, but, for other parameter values, the parasitic behavior, to which multivalue methods are prone, corrupts the numerical solution by the growth of small perturbations. Two approaches for alleviating this effect are considered. First, compositions of methods with growth parameters of opposite signs can be used to cancel the long-term effect of parasitism. Second, methods can be constructed for which the growth parameters are zero by design. Each of these remedies is found to be successful in eliminating parasitic behavior in long-term simulations using a variety of test problems.

Key words. general linear methods, symplectic, parasitism

AMS subject classifications. 65L05, 65L07, 65L20

DOI. 10.1137/140953277

1. Introduction.

G-symplectic general linear methods are a class of multistage multivalue methods designed to numerically solve Hamiltonian differential equations. As we show here, such methods can integrate the solutions of general nonseparable Hamiltonian problems efficiently, and in such a way that energy and symplectic invariants are approximately preserved over long time intervals. In particular, we address the question of controlling parasitic effects, which afflicted early attempts at such methods.

In addition to being energy-preserving, Hamiltonian systems possess what is known as the *symplectic* property. Symplecticity means that the variational equation conserves quadratic quantities [1, 21]. For celestial mechanics, one aspect of symplecticity corresponds to the invariance of angular momentum. A numerical method is called symplectic if it satisfies the discrete analogue of this property. The desirability of a numerical method that is almost exactly symplectic and energy–preserving is clear, especially for computations over a long time.

Only a one-step method can be symplectic in a literal sense [17, 20, 23, 24]. However, every stage of an irreducible symplectic Runge–Kutta method is necessarily implicit [20]. The most efficient such methods are Diagonally Implicit Runge–Kutta methods (DIRKs). It was shown in [22] that all such methods are compositions of the implicit midpoint method. High order composition DIRKs, primarily for time-symmetric problems, were developed in [25, 27, 18]. For separable Hamiltonian problems originating from a system of second order differential equations, the

*Received by the editors January 17, 2014; accepted for publication May 12, 2014; published electronically October 14, 2014.
http://www.siam.org/journals/sinum/52-5/95327.html
†Department of Mathematics, University of Auckland, Auckland 1142, New Zealand (butcher@math.auckland.ac.nz).
‡School of Natural Sciences, National University of Sciences and Technology, H-12, Islamabad, Pakistan (yhabib@sns.nust.edu.pk).
§Department of Mathematical Sciences, University of Bath, Bath BA2 7AY, United Kingdom (masath@bath.ac.uk, tjtn20@bath.ac.uk).

symplectic Euler and Runge–Kutta–Nyström methods have been generalized to obtain higher order partitioned Runge–Kutta methods [15], some of which are explicit. The most popular low order method for separable problems is the explicit Verlet method [26], which may be viewed as a partitioned Runge–Kutta method, a partitioned linear multistep method, or a nonstandard implementation of the leapfrog method.

Conservation properties of standard linear multistep methods were investigated by Eirola and Sanz-Serna [10], who showed that all time-symmetric methods have the G-symplectic property. Although dimensional incommensurability implies that such methods cannot be symplectic themselves, Hairer [12] showed that the underlying one-step method of a symmetric linear multistep method posesses a property similar to symplecticity using a general result on *conjugate symplecticity* proved in [7]. A related question for G-symplectic general linear methods is whether their underlying one-step method is also conjugate symplectic. Although this question remains open theoretically, analogy with the linear multistep case and the computational evidence of section 2.3 suggest that the answer is affirmative.

Unfortunately for multivalue methods, a well-behaved underlying one-step method is insufficient to ensure that the method is effective. A second requirement is that the growth of parasitic components is controlled. However, G-symplecticity implies that the parasitic eigenvalues $\zeta_j(z)$ are unimodular for $z = 0$. Indeed, for the case of linear multistep methods, the parasitic growth parameters $\mu_j = \sigma(\zeta_j)/(\zeta_j\rho'(\zeta_j))$ [8] are nonzero [14, Chapter XIV], leading to numerical instability for many problems of interest. Thus, standard linear symmetric multistep methods have limited applicability. More promisingly, in the case of s-stable time-symmetric linear multistep methods for second order differential equations [13], backward error analysis techniques have been used to show that parasitic components remain under control over long times, so that the numerical solution is largely determined by the well-behaved principal component of the solution. Higher order versions of these methods are applied and analyzed in [19, 15].

G-symplectic general linear methods face hazards from their parasitic components similar to those encountered by standard linear multistep methods. In this paper we consider two distinct approaches to controlling parasitism. First, for the case of a two-step method for which there is one nonzero parasitic component, we compose two numerical methods with growth parameters of opposite signs in such a way that the overall effects cancel out over a long time. This approach is applied to two related fourth order methods. Second, we construct G-symplectic general linear methods for which all parasitic growth parameters are zero. The effectiveness of these two approaches in approximately preserving energy and symplectic invariants over long times is demonstrated by a number of computations.

The new methods constructed here are of up to order 4 and diagonally implicit with, in some cases, extra zeros on the diagonal. As they are designed for *general* Hamiltonian problems, they are in direct competition with symplectic DIRKs. Their construction and analysis depends on simplifications and developments in Diagonally Implicit Multistage Integration method (DIMSIM) general linear methods over the past two decades, especially methods designed for stiff dissipative problems [2, 6, 3].

The paper is organized as follows. In section 2, G-symplectic general linear methods are introduced, and this is followed in section 3 by an account of their parasitic behavior. In section 4, composition of methods is considered as an approach to overcoming the damaging effects of parasitism. In section 5, methods are constructed

in which the parasitic growth parameters are zero by design. Finally, in section 6, numerical simulations are considered as a means of assessing the possible success of our approach to achieving parasitism-free numerical behavior.

2. G-symplectic methods for Hamiltonian systems.

2.1. Invariants and Hamiltonian systems.

Consider an initial value problem

$$y'(x) = f(y(x)), \quad x \in \mathbb{R}, \qquad y(x_0) = y_0 \in \mathbb{R}^N, \qquad f : \mathbb{R}^N \to \mathbb{R}^N. \tag{2.1}$$

Associated with this problem is the variational equation

$$Y'(x) = f'(y(x))Y(x), \qquad Y(x_0) = I, \tag{2.2}$$

where the value of $Y(x)$ at any point x is an $N \times N$ matrix. We will consider the possible existence of invariants for either of these problems. Let $\mathcal{I} : \mathbb{R}^N \to \mathbb{R}$ denote an invariant of the problem (2.1) so that $\mathcal{I}'(y)f(y) = 0$. In particular, we consider the case of quadratic invariants of the form

$$\mathcal{I}(y) = y^{\intercal} Q y$$

for Q a real symmetric $N \times N$ matrix. In this case, it is convenient to define the following bilinear form on $\mathbb{R}^N$:

$$[y, z]_Q := y^{\intercal} Q z, \qquad y, z \in \mathbb{R}^N.$$

For invariance of $[y(x), y(x)]_Q$, we require $[y, f(y)]_Q = 0$ for all $y \in \mathbb{R}^N$.

We recall that an autonomous Hamiltonian system consists of a twice continuously differentiable Hamiltonian $H : \mathbb{R}^{2d} \times \mathbb{R}^{2d} \to \mathbb{R}$, together with generalized momenta $p(x) \in \mathbb{R}^d$ and positions $q(x) \in \mathbb{R}^d$ satisfying the system of differential equations

$$\frac{dp_i}{dx} = -\frac{\partial H}{\partial q_i}, \quad \frac{dq_i}{dx} = \frac{\partial H}{\partial p_i}, \quad i = 1, \ldots, d, \qquad x \in \mathbb{R}. \tag{2.3}$$

Such systems arise in mechanics and several other branches of physics, where H typically corresponds to the sum of kinetic and potential energies.

If we write $y = p \oplus q \in \mathbb{R}^N$, where $N = 2d$, and reinterpret H as a function of y, then (2.3) may be written as

$$\frac{dy}{dx} = J^{-1} \nabla H(y) =: f(y), \tag{2.4}$$

where $\nabla H = (H')^{\intercal}$ is the gradient of H and

$$J = \begin{bmatrix} 0 & I \\ -I & 0 \end{bmatrix} \in \mathbb{R}^{2d \times 2d},$$

where I is the $d \times d$ identity matrix.

Note that $J^{-1} = J^{\intercal} = -J$. Since J is skew-symmetric, it follows that

$$H'(y)f(y) = -(\nabla H)^{\intercal} J (\nabla H) = 0,$$

and hence the Hamiltonian is an invariant.

We will find a *quadratic* invariant of the variational problem associated with (2.4). This problem becomes

$$Y'(x) = \frac{d}{dy}(-J\nabla H)Y(x) = -J\mathbf{H}Y(x), \quad Y(x_0) = I,$$

where $\mathbf{H}$ is the Hessian of H. Note that $\mathbf{H}$ is symmetric.

THEOREM 2.1 (Poincaré). *For any Hamiltonian system,*

$$Y(x)^\intercal JY(x) = J \quad \textit{for all } x \in \mathbb{R}. \tag{2.5}$$

Proof. The identity (2.5) holds at $x = x_0$, and hence it is only necessary to prove that the left-hand side is invariant with x. We have

$$\begin{aligned}\frac{d}{dx}Y(x)^\intercal JY(x) &= Y'(x)^\intercal JY(x) + Y(x)JY'(x)\\ &= -(J\mathbf{H}Y(x))^\intercal JY(x) - Y(x)^\intercal JJ\mathbf{H}Y(x)\\ &= -Y(x)^\intercal\mathbf{H}Y(x) + Y(x)^\intercal\mathbf{H}Y(x) = 0.\end{aligned}$$

This proof is modelled on the one given in [15]. ∎

Equation (2.5) represents what is known as "symplectic behavior." The aim of the present paper is to find reliable methods which approximately preserve quadratic invariants numerically and, as an important special case, preserve symplectic behavior. Although we will not specifically aim to approximately preserve other invariants, we will aim to get as little deviation of H from its initial value as possible for Hamiltonian problems. Currently available symplectic Runge–Kutta methods perform well in this regard, and we will aim for comparable performance in the case of general linear methods.

2.2. General linear methods. We refer to a general linear method (A, U, B, V), where

$$\begin{bmatrix} A & U \\ B & V \end{bmatrix} \tag{2.6}$$

is a partitioned $(s + r) \times (s + r)$ complex-valued matrix or tableau. For practical methods, the coefficients are real, but for some theoretical purposes the complex case is also included in the formulation.

For stepsize $h > 0$, we consider the approximation of the solution of (2.4) for initial data $y_0 \in \mathbb{R}^N$ at the points $x_n := x_0 + nh$, where $n = 0, 1, 2, \ldots$. We assume that a starting method $S_h : \mathbb{R}^N \longrightarrow (\mathbb{R}^N)^r$ generates an initial value $y^{[0]} \in (\mathbb{R}^N)^r$ for the method. Subsequently, new values $y^{[n]} \in (\mathbb{R}^N)^r$ are found from $y^{[n-1]} \in (\mathbb{R}^N)^r$ via the formulae

$$Y = h(A \otimes I)F + (U \otimes I)y^{[n-1]}, \tag{2.7}$$

$$y^{[n]} = h(B \otimes I)F + (V \otimes I)y^{[n-1]}, \tag{2.8}$$

defined using temporary Y, $F \in (\mathbb{R}^N)^s$. The subvectors in F (the stage derivatives) are related to the subvectors in Y (the stages) by $F_i = f(Y_i)$, $i = 1, 2, \ldots, s$. Usually, where there is no ambiguity, the Kronecker products in (2.7) and (2.8) will be omitted and we write

$$\begin{aligned} Y &= hAf(Y) + Uy^{[n-1]},\\ y^{[n]} &= hBf(Y) + Vy^{[n-1]}.\end{aligned} \tag{2.9}$$

In this paper, the method is always assumed to satisfy the following conditions.

DEFINITION 2.2. *A general linear method* (A, U, B, V) *is*

(a) *preconsistent if* $(1, u, w^{\mathsf{H}})$ *is an eigentriple of* V*, such that*

$$Vu = u, \qquad w^{\mathsf{H}}V = w^{\mathsf{H}}, \qquad w^{\mathsf{H}}u = 1;$$

(b) *consistent if it is preconsistent,* $Uu = \mathbf{1}$*, and there exists nonzero* $v \in \mathbb{C}^r$ *such that* $B\mathbf{1} + Vv = u + v$*;*

(c) *zero-stable if* $\sup_{n\geq 0} \|V^n\| < \infty$.

These properties are necessary and sufficient for "convergence" which has a similar meaning to convergence in the case of linear multistep methods.

Let M_h represent the mapping $y^{[n-1]} \mapsto y^{[n]}$. If $y_0 \in \mathbb{R}^N$ is initial data for (2.4), let S_h represent the mapping of y_0 to $y^{[0]} \in (\mathbb{R}^N)^r$, the initial data for the method. Then, M_h is of order $p \in \mathbb{N}$ relative to S_h if

$$S_h(E_h(y_0)) = M_h(S_h(y_0)) + O(h^{p+1}), \tag{2.10}$$

where E_h represents a time-h evolution by the ODE system (2.4). Iterating (2.10), we find

$$S_h(E_{nh}(y_0)) = M_h^n(S_h(y_0)) + O(C(nh)h^p),$$

where C denotes some positive function $C : (0, \infty) \longrightarrow (0, \infty)$. Let F_h, the finishing method, satisfy $F_h(S_h(y)) = y$ for $y \in \mathbb{R}^N$. Then,

$$E_{nh}y_0 - F_h(M_h^n(S_h(y_0))) = O(C(nh)h^p). \tag{2.11}$$

2.3. *G*-symplecticity. A one-step method generates $y_n \approx y(x_n)$, $n \in \mathbb{N}$. It is the purpose of symplectic one-step methods to preserve the value of $[y_n, y_n]_Q$ as n increases.

For a general linear method (2.9), it is necessary to work in the higher dimensional space $(\mathbb{R}^N)^r$, and we consider the possible preservation of $[y^{[n]}, y^{[n]}]_{G\otimes Q}$, where the bilinear form $[\cdot, \cdot]_{G\otimes Q}$ is defined by

$$[y, z]_{G\otimes Q} := \sum_{i,j=1}^{r} g_{ij}[y_i, z_j]_Q, \qquad y, z \in (\mathbb{R}^N)^r, \qquad y_1, \ldots, y_r \in \mathbb{R}^N,$$

for Hermitian nonsingular $G \in \mathbb{C}^{r\times r}$. It is known [15] that the conditions for $[y^{[n]}, y^{[n]}]_{G\otimes Q}$ to be invariant are that there exists a real diagonal $s \times s$ matrix D such that

$$M := \begin{bmatrix} DA + A^{\mathsf{T}}D - B^{\mathsf{H}}GB & DU - B^{\mathsf{H}}GV \\ U^{\mathsf{H}}D - V^{\mathsf{H}}GB & G - V^{\mathsf{H}}GV \end{bmatrix} = 0. \tag{2.12}$$

Note that, even if the coefficient matrices U, B, V are real, they may become complex under a complex coordinate transformation $U \mapsto UT$, $B \mapsto T^{-1}B$, $V \mapsto T^{-1}VT$. However, A is invariant with respect to this change of coordinates. In particular, if A is real, as it will be for a practical method, it will remain real in a transformed method.

As an initial example of a G-symplectic method, we consider the following method, introduced in [4]:

$$\left[\begin{array}{cc|cc} \frac{3+\sqrt{3}}{6} & 0 & 1 & -\frac{3+2\sqrt{3}}{3} \\ -\frac{\sqrt{3}}{3} & \frac{3+\sqrt{3}}{6} & 1 & \frac{3+2\sqrt{3}}{3} \\ \hline \frac{1}{2} & \frac{1}{2} & 1 & 0 \\ \frac{1}{2} & -\frac{1}{2} & 0 & -1 \end{array}\right]. \tag{2.13}$$

The method (2.13) satisfies the G-symplectic conditions with

$$G = \begin{bmatrix} 1 & 0 \\ 0 & \frac{3+2\sqrt{3}}{3} \end{bmatrix}, \qquad D = \begin{bmatrix} \frac{1}{2} & 0 \\ 0 & \frac{1}{2} \end{bmatrix}.$$

The method M_h defined by (2.13) has order 4 relative to the starting method S_h, defined by

$$S_h(y_0) := \begin{bmatrix} y_0 \\ \frac{1}{2}(R_h y_0 + R_{-h} y_0) - y_0 \end{bmatrix}, \tag{2.14}$$

where R_h is the Runge–Kutta method, written as a general linear method with $r = 1$:

$$\left[\begin{array}{cccc|c} 0 & 0 & 0 & 0 & 1 \\ \frac{1}{2} & 0 & 0 & 0 & 1 \\ \frac{5}{11} & \frac{6}{11} & 0 & 0 & 1 \\ \frac{9-\sqrt{3}}{72} & -\frac{15+2\sqrt{3}}{54} & \frac{33+11\sqrt{3}}{216} & 0 & 1 \\ \hline 0 & \frac{10\sqrt{3}}{27} & -\frac{11\sqrt{3}}{108} & 1 & 1 \end{array}\right]. \tag{2.15}$$

To see that the method is indeed of order 4, we first note that the B-series coefficients in the second component of S_h can be found from the elementary weights of R_h. In the present section only, G will denote the generalization of the Runge–Kutta group introduced in [4, subsection 385]. We find for $\xi \in G^2$, representing the input, that

$$\xi(\emptyset) = \begin{bmatrix} 1 \\ 0 \end{bmatrix}, \ \xi(\bullet) = \begin{bmatrix} 0 \\ 0 \end{bmatrix}, \ \xi(\!\!\begin{array}{c}\bullet\\|\end{array}\!\!) = \begin{bmatrix} 0 \\ \frac{\sqrt{3}}{12} \end{bmatrix}, \ \xi(\!\!\begin{array}{c}\bullet\\|\\\bullet\end{array}\!\!) = \begin{bmatrix} 0 \\ 0 \end{bmatrix}, \ \xi(\!\!\begin{array}{c}\bullet\\|\\\bullet\end{array}\!\!) = \begin{bmatrix} 0 \\ 0 \end{bmatrix},$$

$$\xi(\!\!\begin{array}{c}\bullet\\|\\\bullet\end{array}\!\!) = \begin{bmatrix} 0 \\ -\frac{\sqrt{3}}{18} \end{bmatrix}, \ \xi(\!\!\begin{array}{c}\bullet\\|\\\bullet\end{array}\!\!) = \begin{bmatrix} 0 \\ -\frac{\sqrt{3}}{36} \end{bmatrix}, \ \xi(\!\!\begin{array}{c}\bullet\\|\\\bullet\end{array}\!\!) = \begin{bmatrix} 0 \\ \frac{3+\sqrt{3}}{36} \end{bmatrix}, \ \xi(\!\!\begin{array}{c}\bullet\\|\\\bullet\end{array}\!\!) = \begin{bmatrix} 0 \\ \frac{3+\sqrt{3}}{72} \end{bmatrix}.$$

Thus ξ agrees with the value given in Table 534(I) in [4] and, from the agreement between the last two lines of this table, as far as order 4, with the values of $E\xi$, the method is seen to have order 4.

The method (2.13) will be referred to as P, and a similar method, in which the sign of $\sqrt{3}$ is reversed, will be referred to as N.

3. Parasitic behavior in G-symplectic methods. To illustrate the approximate conservation properties of these methods, we will consider the use of (2.13) to solve the simple pendulum problem based on the Hamiltonian

$$H = \frac{p^2}{2} - \cos(q).$$

For consistency of notation, we will identify p and q with y_1 and y_2, respectively, and we get the differential equation system

$$\begin{aligned} y_1' &= -\sin(y_2), \\ y_2' &= y_1. \end{aligned}$$

For our numerical experiments, the initial value is given by $y = [0, 1.2]^{\mathsf{T}}$, that is, the amplitude is 1.2. Implementing method P with $h = 0.01$ over 10^6 time steps yields Figure 1, which plots $H(y_n)$ against x, where $y_n = F_h(M_h^n(S_h(y_0)))$ for $nh = x$. The results of a number of computations indicate that this is typical behavior for a G-symplectic method in the absence of parasitism. Such numerical experiments, combined with the theoretical results of [9] showing the existence of a conjugate symplectic underlying one-step method for a G-symplectic method, lead us to believe that G-symplecticity is an important property for general linear methods approximating conservative problems.

Later, in Figure 3, we will observe parasitism for method P, when the amplitude is sufficiently large for the eigenvalues of the Jacobian matrix to change from imaginary to real during the computation.

We see in Figure 2, that the behavior is very similar when method N is used instead of method P. Although there is no sign of excessive deviation from the initial value of the numerical Hamiltonian, for the low amplitude experiments shown in Figures 1 and 2, an increase in the amplitude can make a significant difference. In anticipation of this changed behavior, the scales for the vertical axes are nonlinear and are based on transformations of the form $y \mapsto \operatorname{sgn}(y)\log(1 + a|y|)$ for suitably chosen a. This applies to all figures here and in section 3. An extension of this experiment, in which 10^6 time steps were performed, showed no deviation from this type of behavior.

However, when the amplitude is increased to 1.76, there is a complete change in the nature of the results, caused by the build-up of the parasitic component. These are shown in Figure 3. For method N the damaging effect of parasitism with this

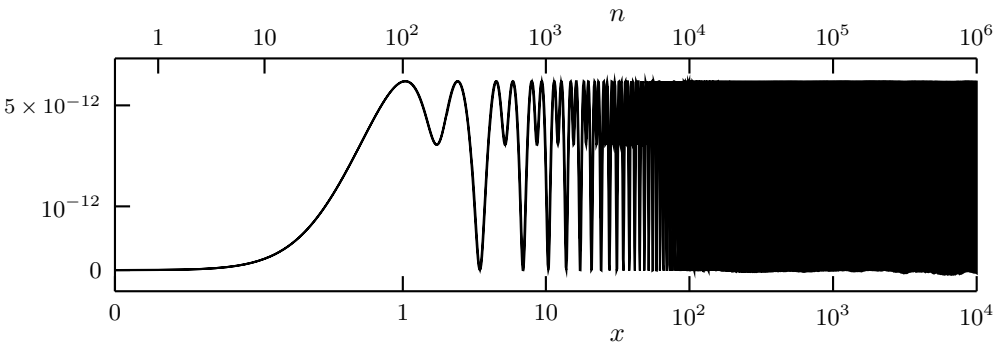

FIG. 1. *The variation in the numerical Hamiltonian for the simple pendulum problem with initial value* $y = [0, 1.2]^{\mathsf{T}}$*, using method* P *and* 10^6 *steps with* $h = 0.01$.

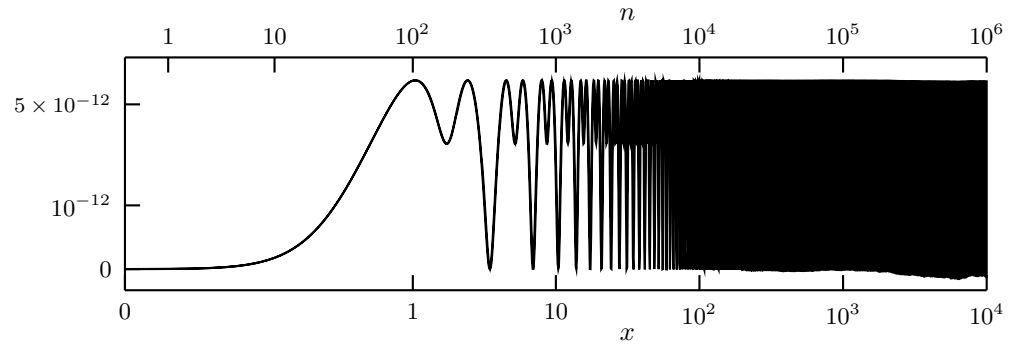

FIG. 2. *The variation in the numerical Hamiltonian for the simple pendulum problem with initial value* $y = [0, 1.2]^{\mathsf{T}}$*, using method* N *and* $h = 0.01$.

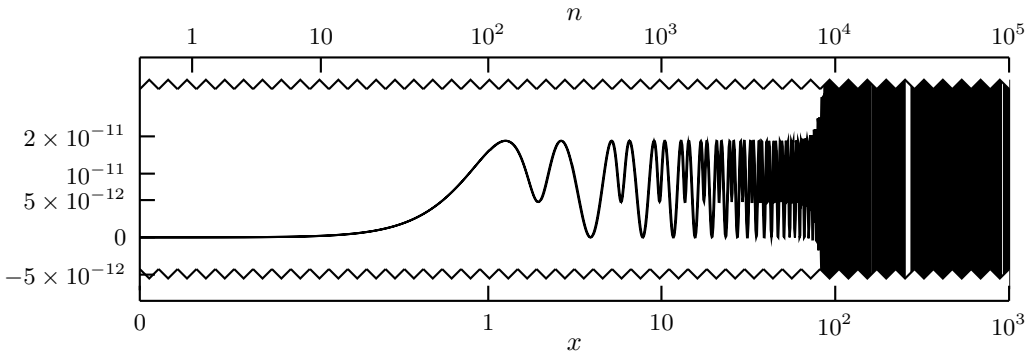

FIG. 3. *The variation in the numerical Hamiltonian for the simple pendulum problem with initial value* $y = [0, 1.76]^{\mathsf{T}}$*, using method* P *with* $h = 0.01$.

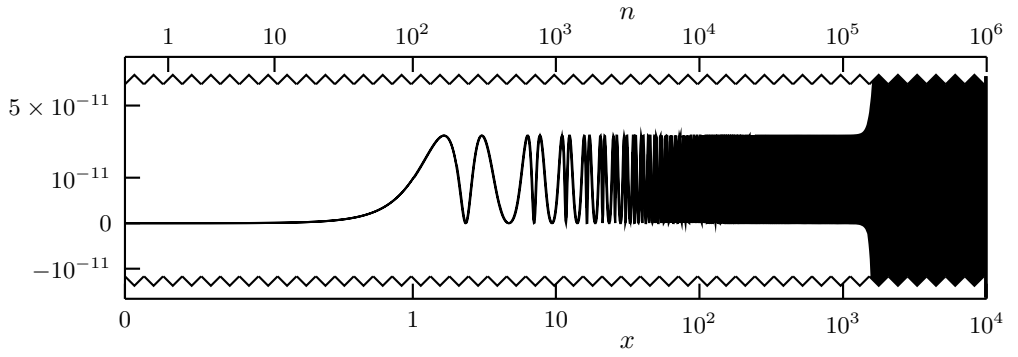

FIG. 4. *The variation in the numerical Hamiltonian for the simple pendulum problem with initial value of* $y = [0, 2.3]^{\mathsf{T}}$*, using method* N *with* $h = 0.01$.

stepsize is not observed within the first million steps unless the amplitude is increased above 1.76. For amplitude 2.3, on the other hand, the disastrous effect of parasitism becomes apparent after approximately 1.6×10^5 steps. This behavior is shown in Figure 4.

Following [15], we explain why parasitism occurs, at least for large amplitudes. It is typical of multivalue methods to suffer from corruption by parasitic components

because perturbations to the nonprincipal components can become magnified as the integration proceeds.

We consider a typical step of the general linear method

$$\begin{bmatrix} Y_1 \\ Y_2 \\ \hline y_1^{[n]} \\ y_2^{[n]} \end{bmatrix} = \left[\begin{array}{cc|cc} a_{11} & a_{11} & u_{11} & u_{12} \\ a_{21} & a_{22} & u_{21} & u_{22} \\ \hline b_{11} & b_{12} & 1 & 0 \\ b_{21} & b_{22} & 0 & -1 \end{array}\right] \begin{bmatrix} hF_1 \\ hF_2 \\ \hline y_1^{[n-1]} \\ y_2^{[n-1]} \end{bmatrix},$$

where we note that V has eigenvalues 1 and -1. The stages and output values are given by

$$\begin{aligned} Y_i &= h\sum_{j=1}^{2} a_{ij}F_j + u_{i1}y_1^{[n-1]} + u_{i2}y_2^{[n-1]}, \qquad i = 1, 2, \\ y_1^{[n]} &= h\sum_{i=1}^{2} b_{1i}F_i + y_1^{[n-1]}, \\ y_2^{[n]} &= h\sum_{i=1}^{2} b_{2i}F_i - y_2^{[n-1]}. \end{aligned}$$

While the first component $y_1^{[n]}$ approximates the exact solution, the second component $y_2^{[n]}$ approximates a related quantity such as the scaled second derivative, as in the case of (2.13). To see how the value of $y_2^{[n]}$ can cause parasitic behavior, consider what happens when a perturbation is introduced at the start of step n:

$$y_2^{[n-1]} \longrightarrow y_2^{[n-1]} + (-1)^{n-1}z_{n-1}.$$

This perturbation will affect the stages Y_i approximately as

$$Y_i + \delta Y_i = h\sum_{j=1}^{2} a_{ij}F_j + u_{i1}y_1^{[n-1]} + u_{i2}(y_2^{[n-1]} + (-1)^{n-1}z_{n-1}),$$

so that $\delta Y_i \approx (-1)^{n-1}u_{i2}z_{n-1}$, and this will in turn cause the stage derivative F_i to be perturbed by

$$F_i \longrightarrow F_i + \delta F_i = f(Y_i + \delta Y_i),$$

where $\delta F_i \approx (-1)^{n-1}\frac{\partial f}{\partial y}u_{i2}z_{n-1}$. The effect of these perturbations, for $i = 1, 2, \ldots, s$, on the second output value is

$$y_2^{[n]} \longrightarrow y_2^{[n]} + (-1)^n z_n,$$

where

$$\begin{aligned} (-1)^n z_n &\approx -(-1)^{n-1}z_{n-1} - h\sum_{i=1}^{2} b_{2i}\delta F_i y_2^{[n]} \\ &= (-1)^n z_{n-1} + (-1)^{n-1}h\sum_{i=1}^{2} b_{2i}u_{i2}\frac{\partial f}{\partial y}z_{n-1}, \end{aligned}$$

so that

$$z_n \approx \left(1 - h\sum_{i=1}^{2} b_{2i}u_{i2}\frac{\partial f}{\partial y}\right) z_{n-1}.$$

This is approximately the Euler method applied to the differential equation,

$$z' = \mu\frac{\partial f}{\partial y} z, \tag{3.1}$$

where $\mu = -\sum_{i=1}^{2} b_{2i}u_{i2}$ is the growth parameter for the parasitic component z_n. In matrix terms, μ can be found from the matrix product,

$$BU = \begin{bmatrix} 1 & 0 \\ 0 & -\mu \end{bmatrix}.$$

To get an idea of the growth rates of methods P and N, we evaluate μ for these two methods; the results are, respectively,

$$\begin{aligned} \mu_P &= 1 + \frac{2\sqrt{3}}{3} = 2.154700538379251, \\ \mu_N &= 1 - \frac{2\sqrt{3}}{3} = -0.154700538379251. \end{aligned} \tag{3.2}$$

In section 4, we will see how to exploit the opposite signs of growth parameters μ_P and μ_N to cancel out parasitism. But ultimately, our aim will be to construct methods for which $\mu = 0$ with the hope of eliminating parasitic behavior entirely.

4. Using compositions to annihilate parasitism.

4.1. Cancellation by interspersing alternative methods. Consider two G-symplectic methods M_h and $\widehat{M}_h$ with respective coefficient matrices (A, U, B, V) and $(\widehat{A}, \widehat{U}, \widehat{B}, \widehat{V})$. The composition $\widetilde{M}_{2h} := \widehat{M}_h \circ M_h$ has tableau

$$\begin{bmatrix} \widetilde{A} & \widetilde{U} \\ \widetilde{B} & \widetilde{V} \end{bmatrix} = \left[\begin{array}{cc|c} A & 0 & U \\ \widehat{U}B & \widehat{A} & \widehat{U}V \\ \hline \widehat{V}B & \widehat{B} & \widehat{V}V \end{array}\right]. \tag{4.1}$$

Below, we prove a restricted version of a more general result on the additivity of parasitic growth parameters.

THEOREM 4.1. *Let the above assumptions hold with $V = \widehat{V} = \mathrm{diag}(1, -1)$. Let the growth parameters of M_h and $\widehat{M}_h$ be μ and $\widehat{\mu}$, respectively. The growth parameter for $\widetilde{M}_h := \widehat{M}_h \circ M_h$ satisfies*

$$\widetilde{\mu} = \mu + \widehat{\mu}. \tag{4.2}$$

Proof. Evaluate

$$\widetilde{B}\widetilde{U} = \widehat{V}BU + \widehat{B}\widehat{U}V. \tag{4.3}$$

Since $\widetilde{V} = \widehat{V}V = I_2$,

$$\widetilde{\mu} = e_2^{\intercal}\widetilde{B}\widetilde{U}e_2 = -e_2^{\intercal}BUe_2 - e_2^{\intercal}\widehat{B}\widehat{U}e_2 = \mu + \widehat{\mu}. \tag{4.4}$$

∎

Recall (3.2) that the growth parameters μ_P and μ_N have opposite signs. This, together with the additivity property proved above, suggests that parasitic effects may be cancelled by an appropriate composition of P and N. However, for this to work in practice, we use a linear change of basis to transform N so that the modified N has a starting method more similar to that of P but still retains the same value of μ_N. Below, we give the tableau for the modified N; the P tableau is also given for comparison:

$$P: \left[\begin{array}{cc|cc} \frac{3+\sqrt{3}}{6} & 0 & 1 & -\frac{3+2\sqrt{3}}{3} \\ -\frac{\sqrt{3}}{3} & \frac{3+\sqrt{3}}{6} & 1 & \frac{3+2\sqrt{3}}{3} \\ \hline \frac{1}{2} & \frac{1}{2} & 1 & 0 \\ \frac{1}{2} & -\frac{1}{2} & 0 & -1 \end{array}\right], \qquad N: \left[\begin{array}{cc|cc} \frac{3-\sqrt{3}}{6} & 0 & 1 & \frac{3-2\sqrt{3}}{3} \\ \frac{\sqrt{3}}{3} & \frac{3-\sqrt{3}}{6} & 1 & -\frac{3-2\sqrt{3}}{3} \\ \hline \frac{1}{2} & \frac{1}{2} & 1 & 0 \\ -\frac{1}{2} & \frac{1}{2} & 0 & -1 \end{array}\right].$$

It will be noted that these tableaux seem to be related by changing the sign of $\sqrt{3}$. However, the linear transformation which modifies N also changes the signs of u_{12}, u_{22}, b_{21}, b_{22}. This corresponds to a change of sign of the input and output components $y_2^{[n-1]}$ and $y_2^{[n]}$ and makes it appropriate to compose N and P without any adjustment since, for both methods,

$$\begin{aligned} y_1^{[n]} &= y(x_n) + O(h^5), \\ y_2^{[n]} &= h^2 \frac{\sqrt{3}}{12} y''(x_n) + O(h^4). \end{aligned} \tag{4.5}$$

A suitable input for $y^{[0]}$ to achieve this accuracy is provided by the starting method (2.14) proposed for method P, but with (2.15) replaced by

$$\left[\begin{array}{cccc|c} 0 & 0 & 0 & 0 & 1 \\ \frac{1}{2} & 0 & 0 & 0 & 1 \\ \frac{5}{11} & \frac{6}{11} & 0 & 0 & 1 \\ \frac{9+\sqrt{3}}{72} & -\frac{15-2\sqrt{3}}{54} & \frac{33-11\sqrt{3}}{216} & 0 & 1 \\ \hline 0 & \frac{10\sqrt{3}}{27} & -\frac{11\sqrt{3}}{108} & -1 & 1 \end{array}\right].$$

The results of section 3 showed that both N and P conserve the Hamiltonian to high accuracy over long times in the absence of parasitism. We therefore expect that compositions of N and P will similarly conserve the Hamiltonian, provided that parasitism is annihilated. Below, we consider how to compose N and P to achieve this annihilation:

As at the end of section 3, an evaluation of $\mu = -e_2^{\mathsf{T}} B U e_2$ gives

$$\begin{aligned} \mu &= 1 + \frac{2\sqrt{3}}{3} = 2.154700538379251 \quad \text{for method } P, \\ \mu &= 1 - \frac{2\sqrt{3}}{3} = -0.154700538379251 \quad \text{for method } N. \end{aligned}$$

A first composition based approach to controlling parasitism is to use N for most steps but, occasionally, to insert a step using P. If after n steps, N has been used $n-m$ times and P has been used m times, the accumulated total of μ values will be $n-(n-2m)\frac{2\sqrt{3}}{3}$. By choosing an appropriate sequence, it is possible to maintain a value of this accumulated total in the interval $[-\frac{2\sqrt{3}}{3}, \frac{2\sqrt{3}}{3}]$. This gives a sequence which starts as follows:

$$N^7\ P\ N^{14}\ P\ N^{14}\ P\ N^{14}\ P\ N^{14}\ P\ N^{14}\ P\ N^{14}\ P\ N^{13}\ P\cdots.$$

To test the suitability of this sequence two experiments using the simple pendulum are presented. In each case 10^6 steps are performed using a stepsize $h = 0.01$. These are shown for a moderate amplitude case ($p_0 = 0$, $q_0 = 1.2$) in Figure 5 and for a high amplitude case ($p_0 = 0$, $q_0 = 3$) in Figure 6.

The observed deterioration of behavior in Figures 5 and 6 is a strong argument against the use of the $N^7PN^{14}P\cdots$ sequence.

We will now present an explanation of this behavior and show how the situation can be significantly improved by using an alternative sequence.

As we have remarked, to obtain order 4 output from the first component of each step of the N^7P sequence, it is enough that the input to the step satisfies (4.5). However, to satisfy the formal definition of order, the second component of the starting methods for N and P are equal to be ξ_N and ξ_P, where, for various trees up to order

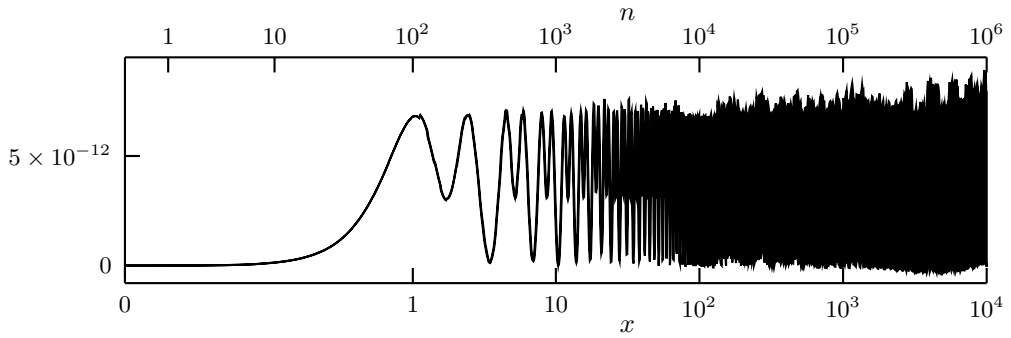

FIG. 5. *$H - H_0$ for simple pendulum using $N^7PN^{14}P\cdots$ with initial value $y = [0, 1.2]^{\intercal}$ and stepsize $h = 0.01$.*

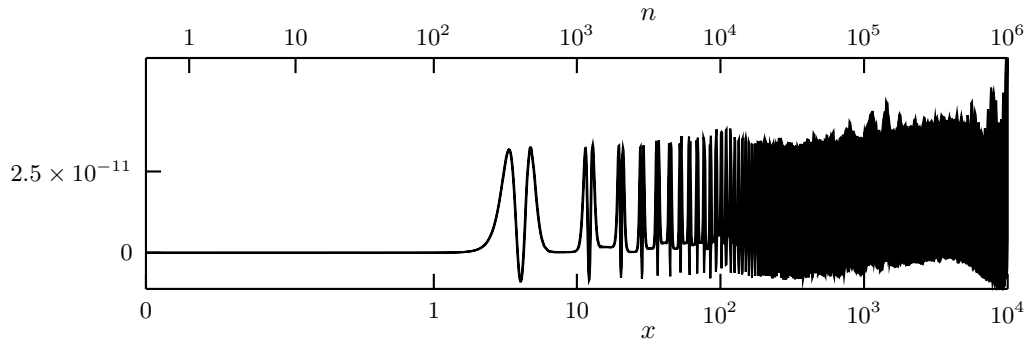

FIG. 6. *$H - H_0$ for simple pendulum using $N^7PN^{14}P\cdots$ with initial value $y = [0, 3]^{\intercal}$ and stepsize $h = 0.01$.*

4, $\xi_N(t)$ and $\xi_P(t)$ are given in (4.6). The additional entry $\widehat{\xi}(a)(t)$ will be explained below.

(4.6)

t	$\emptyset$	$\bullet$							
$\xi_N(t)$	0	0	$\frac{\sqrt{3}}{12}$	0	0	$-\frac{\sqrt{3}}{18}$	$-\frac{\sqrt{3}}{36}$	$\frac{\sqrt{3}}{36}-\frac{1}{12}$	$\frac{\sqrt{3}}{72}-\frac{1}{24}$
$\xi_P(t)$	0	0	$\frac{\sqrt{3}}{12}$	0	0	$-\frac{\sqrt{3}}{18}$	$-\frac{\sqrt{3}}{36}$	$\frac{\sqrt{3}}{36}+\frac{1}{12}$	$\frac{\sqrt{3}}{72}+\frac{1}{24}$
$\widehat{\xi}(a)(t)$	0	0	$\frac{\sqrt{3}}{12}$	0	0	$-\frac{\sqrt{3}}{18}$	$-\frac{\sqrt{3}}{36}$	$\frac{\sqrt{3}}{36}+\frac{a}{12}$	$\frac{\sqrt{3}}{72}+\frac{a}{24}$

From these functions we see that $\xi_P = \widehat{\xi}(1)$ and that $\xi_N = \widehat{\xi}(-1)$. Suppose the input component to step number n are $y_1^{[n-1]}$ and $y_2^{[n-1]} = B(\widehat{\xi}(a_{n-1}), y_1^{[n-1]})$, where the expression for $y_2^{[n-1]}$ denotes a B-series. In this case, to within order $O(h^5)$, the outputs will be $y_1^{[n]}$, say, and $y_2^{[n]} = B(\widehat{\xi}(a_n), y_1^{[n]})$, where

$$a_n = \begin{cases} -2 - a_{n-1} & \text{if step } n \text{ uses method N,} \\ 2 - a_{n-1} & \text{if step } n \text{ uses method P.} \end{cases} \tag{4.7}$$

If the NP sequence is known, and $a_0 = -1$, corresponding to a starting method appropriate for method N, then (4.7) determines a sequence $(a_0, a_1, a_2, \ldots)$. We want to know if this is a bounded sequence because, if this were the case, there would be no source of unstable behavior caused by frequent switches between N and P. However, an analysis of the sequence generated by $N^7PN^{14}P\cdots$ indicates that $|a_n|$ grows at rate proportional to 1.00356^n, and this becomes unacceptable for large values of n. This explains the deterioration, for a large number of steps, in the behavior of simulations with the simple pendulum.

These apparent difficulties can be overcome by modifying the sequence to ensure that only *even* numbers of N steps can occur between the occurences of P. After a total of n steps have been performed, let ν_n denote the number of occurences of N from the start or from the last P.

The modified algorithm, for deciding between P and N to be used in step number n, with initial values $\Sigma_0 = 0$, $\nu_0 = 0$, becomes

if $\Sigma_{n-1} > -\left(\frac{3}{2} - \frac{1}{3}\sqrt{3}\right)$ or ν_n is odd, then choose N with

$$\Sigma_n = \Sigma_{n-1} + 1 - \frac{2\sqrt{3}}{3}, \nu_n = \nu_{n-1} + 1,$$

if $\Sigma_{n-1} < -\left(\frac{3}{2} - \frac{1}{3}\sqrt{3}\right)$ and ν_n is even, then choose P with

$$\Sigma_n = \Sigma_{n-1} + 1 + \frac{2\sqrt{3}}{3}, \nu_n = 0.$$

The sequence is now

$$N^6PN^{14}P\cdots,$$

where 27 repetitions of $N^{14}P$ occur before the first appearance of $N^{12}P$. To verify that the modification, of insisting on even numbers of N in sequence, is successful, we present two simulations for comparison with Figures 5 and 6, respectively. The new results are shown in Figures 7 and 8, respectively.

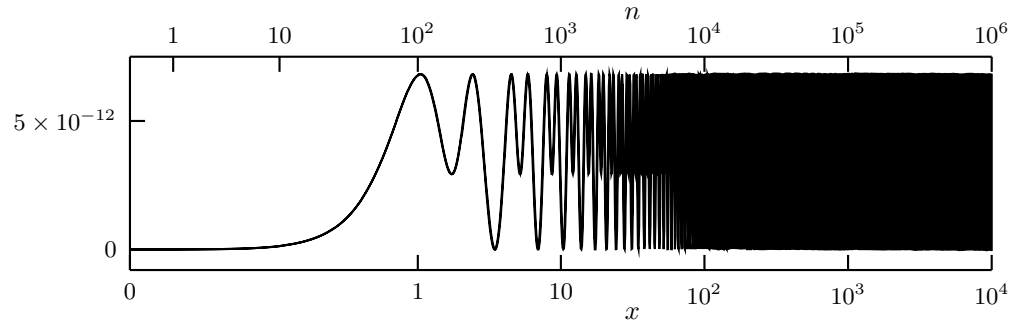

FIG. 7. $H - H_0$ *for* N^6P *sequence with initial value* $y = [0, 1.2]^{\mathsf{T}}$.

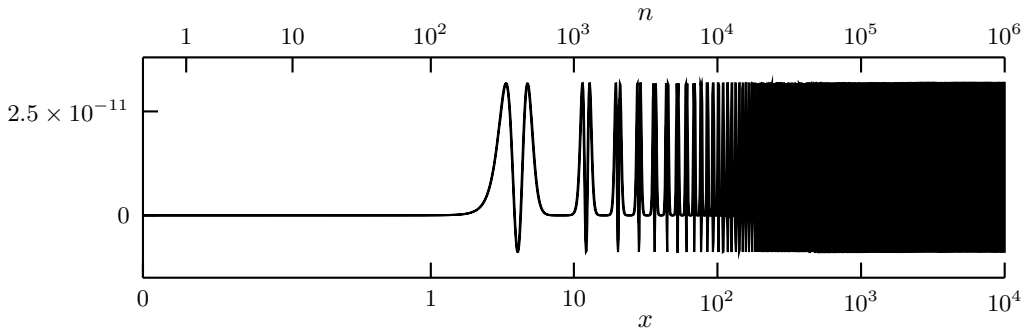

FIG. 8. $H - H_0$ *for* N^6P *sequence with initial value* $y = [0, 3]^{\mathsf{T}}$.

4.2. Cancellation using compositions of scaled steps. Instead of taking a variable number of steps with method N followed by a single step, with the same stepsize, using P, we will, for a specific positive integer m, look at methods which take exactly m steps with N, followed by a single step using P, but with an adjusted stepsize. The adjustment will be chosen so that the sum of the scaled μ values will exactly cancel at the end of the $m + 1$ steps. If the transition from N to P has a stepsize change in the ratio θ, then the total size of the $m + 1$ steps will be $m + \theta$. To obtain a straightforward comparison between different annihilation schemes, we will use h to denote the mean stepsize so that the m steps using N will use stepsize $h/(m + \theta)$ and the single step in each cycle using P will use stepsize $h\theta/(m + \theta)$. To choose the right value of θ, calculate the total of the $\mu \times$ stepsize values in each cycle. This total is

$$\frac{m(1 - \frac{2\sqrt{3}}{3}) + \theta\big(1 + \frac{2\sqrt{3}}{3}\big)}{m + \theta},$$

which becomes zero, for complete annihilation when

$$\theta = m(7 - 4\sqrt{3}).$$

Because the second output has the same value to within $O(h^3)$ for the two methods, if the stepsize is constant, an adjustment will have to be made when we move between them *when the stepsize is not constant.* This means that when a step N has been completed and a step N is about to be taken, with stepsize multiplied by θ, the value of $y_2^{[n]}$ will have to be multiplied by θ^2. Similarly, when the step P has been completed, the corresponding component of the output will have to be multiplied by

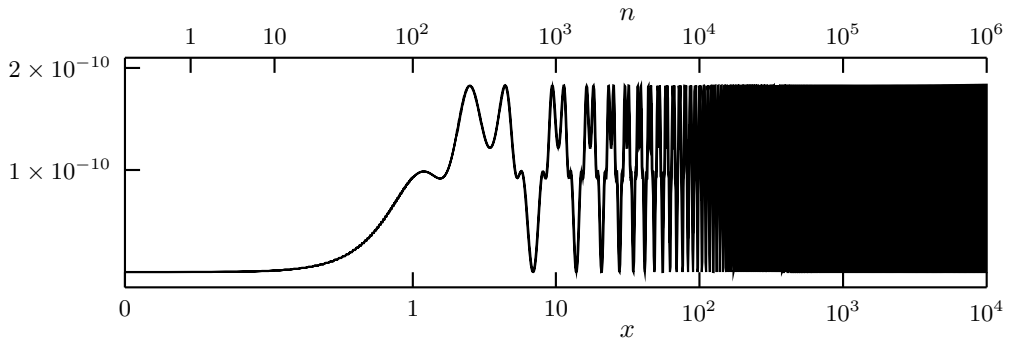

FIG. 9. *Variation in the Hamiltonian for the simple pendulum with initial value* $y = [0, 1.2]^{\mathsf{T}}$, *using the* $N^m P$ *method with* $m = 1$.

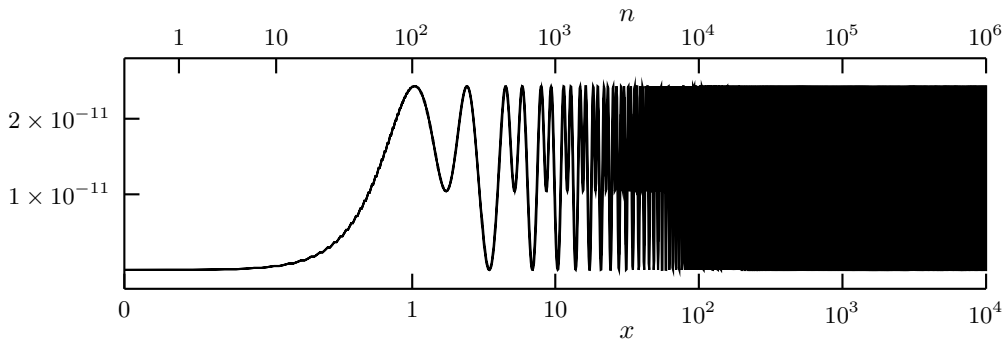

FIG. 10. *Variation in the Hamiltonian for the simple pendulum with initial value* $y = [0, 1.2]^{\mathsf{T}}$, *using the* $N^m P$ *method with* $m = 2$.

θ^{-2}, before the sequence of N steps is taken. In each case, 10^6 steps are taken with stepsize $h = 0.01$.

We will now present a series of experiments with the simple pendulum to see how well this method works for various values of m. First we will show the deviation of the Hamiltonian from its initial value for a low amplitude initial value ($y = [0, 1.2]^{\mathsf{T}}$) in the two cases $m = 1$, in Figure 9, and $m = 2$, in Figure 10. The effect of parasitism is again effectively controlled by the sequence of steps.

The results show a preference for $m = 2$ in that the deviations are an order of magnitude lower than with $m = 1$. To compare other values of m, we will use a simplified type of diagram in which after n steps the value of $\max_{k=1}^{n} |H_k - H_0|$ is shown. This diagram for $m = \{2, 3, 4, 8\}$ is shown in Figure 11.

Finally, in experiments using $N^m P$ methods, we present in Figure 12 the results for a more demanding choice of initial value, $y = [0, 3]^{\mathsf{T}}$, with $m = 8$ and $h = 0.01$.

5. Construction of a method with zero parasitic growth. In this section we will show how a method with order 4 can be constructed, which has zero growth parameters. For efficiency of implementation we will require the coefficient matrix A to be lower triangular with as low a value of s as possible. Although methods with $s = 5$ are available with only three nonzero diagonal elements, we will restrict our consideration to $s = 4$.

5.1. A method with $rs = 24$. The first method we will consider is based on the assumption $r = 2$ with $V = \mathrm{diag}(1, -1)$. It was shown in [5] that time-reversal

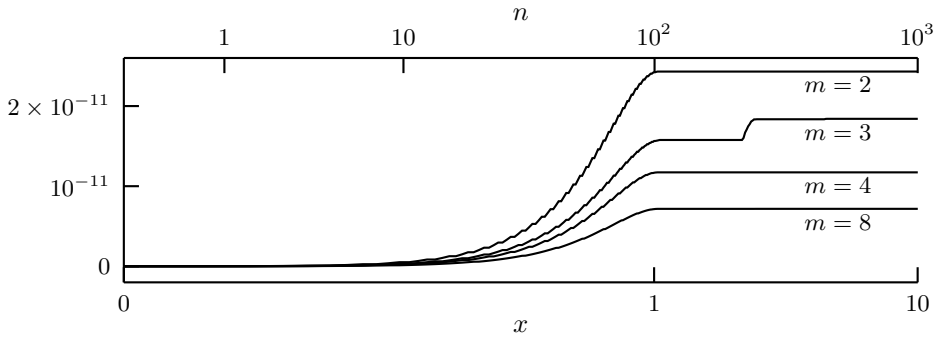

FIG. 11. *Variation in the Hamiltonian for the simple pendulum with initial value* $y = [0, 1.2]^{\mathsf{T}}$ *using the* $N^m P$ *method with* $m = 2, 3, 4, 8$.

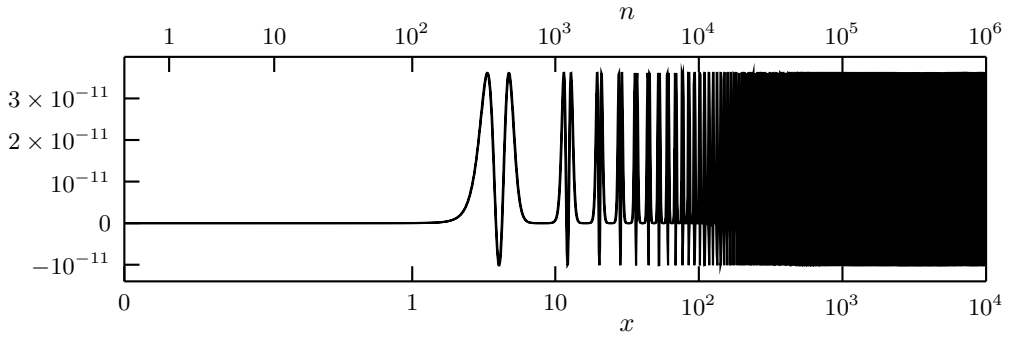

FIG. 12. *Variation in the Hamiltonian for the simple pendulum with initial value* $y = [0, 3]^{\mathsf{T}}$, *using the* $N^m P$ *method with* $m = 8$.

symmetry implies evenness of order. Hence, we will adopt this, as part of our ansatz, so that order 4 can be achieved by requiring only that order 3 conditions are satisfied.

For a symmetric method of the type we are considering, B and U^{T} have the forms

$$B = \begin{bmatrix} b_1 & b_2 & b_2 & b_1 \\ \beta_1 & \beta_2 & \pm\beta_2 & \pm\beta_1 \end{bmatrix}, \quad U^{\mathsf{T}} = \begin{bmatrix} 1 & 1 & 1 & 1 \\ u_1 & u_2 & \pm u_2 & \pm u_1 \end{bmatrix},$$

and we will choose $\pm = -1$. To eliminate parasitism, we must have $\beta_1 u_1 + \beta_2 u_2 = 0$, and by adopting a suitable scaling, we can assume without loss of generality that $\beta_1 = 1$, $\beta_2 = -t$, $u_1 = t$, and $u_2 = 1$. By consistency, $b_1 + b_2 = 1$, and by the condition $DU = B^{\mathsf{T}} GV$ in (2.12), $b_1 t = -g$ and $b_2 = tg$. It now follows that $b_1 = 1/2(1 - t^2)$, $b_2 = -t^2/2(1 - t^2)$, $g = -t/2(1 - t^2)$, and assuming a lower-triangular form for A, we construct this matrix from $DA + A^{\mathsf{T}} D = B^{\mathsf{T}} GB$ in (2.12). The method is now completely known up to the choice of t:

$$\begin{bmatrix} A & U \\ B & V \end{bmatrix} = \left[\begin{array}{cccc|cc} \frac{1-2t+2t^3}{4(1-t^2)} & 0 & 0 & 0 & 1 & t \\ \frac{2t^2-1}{2(1-t^2)} & \frac{t(2-t-2t^2)}{4(1-t^2)} & 0 & 0 & 1 & 1 \\ \frac{3-2t^2}{2(1-t^2)} & \frac{t(-2-t+2t^2)}{2(1-t^2)} & \frac{t(2-t-2t^2)}{4(1-t^2)} & 0 & 1 & -1 \\ \frac{1+2t-2t^3}{2(1-t^2)} & \frac{t^2(-3+2t^2)}{2(1-t^2)} & \frac{t^2(1-2t^2)}{2(1-t^2)} & \frac{1-2t+2t^3}{4(1-t^2)} & 1 & -t \\ \hline \frac{1}{2(1-t^2)} & \frac{-t^2}{2(1-t^2)} & \frac{-t^2}{2(1-t^2)} & \frac{1}{2(1-t^2)} & 1 & 0 \\ 1 & -t & t & -1 & 0 & -1 \end{array}\right].$$

The choice of t will be based on an attempt to obtain order 3 (and therefore, by symmetry, order 4). The starting method will be assumed to be of the form

$$S_h y_0 = \begin{bmatrix} y_0 \\ B(\xi, y_0) \end{bmatrix},$$

where ξ in the B-series defining the second input satisfies $\xi(\emptyset) = 0$ and, by the order condition, $\xi(\bullet) = 0$. Let $B(\eta, y_0)$ and $B(\eta D, y_0)$ denote the B-series for the stage values and stage derivatives, respectively. Then we have

$$\eta(\bullet) = A\mathbf{1} + \xi(\bullet)u = A\mathbf{1} =: c, \tag{5.1}$$

$$\eta(\begin{smallmatrix}\bullet\\\bullet\end{smallmatrix}) = Ac + \xi(\begin{smallmatrix}\bullet\\\bullet\end{smallmatrix})u, \tag{5.2}$$

$$(\eta D)(\begin{smallmatrix}&\bullet\\\bullet&\end{smallmatrix}) = c^2, \tag{5.3}$$

$$(\eta D)(\begin{smallmatrix}\bullet\\\bullet\\\bullet\end{smallmatrix}) = Ac + \xi(\begin{smallmatrix}\bullet\\\bullet\end{smallmatrix})u. \tag{5.4}$$

Because the method is automatically of order at least 2, it is sufficient to choose t such that $b^{\mathsf{T}}(\eta D)(\begin{smallmatrix}&\bullet\\\bullet&\end{smallmatrix}) = \frac{1}{3}$ and $b^{\mathsf{T}}(\eta D)(\begin{smallmatrix}\bullet\\\bullet\\\bullet\end{smallmatrix}) = \frac{1}{6}$. The two order equations are

$$b^{\mathsf{T}}c^2 = \frac{1}{3},$$
$$b^{\mathsf{T}}Ac = \frac{1}{6},$$

where the last equation simplifies because $b^{\mathsf{T}}u = 0$. We are now faced with two equations for t, but these are equivalent because of $DA + A^{\mathsf{T}}D = B^{\mathsf{T}}GB$ in (2.12). Multiply on the left by $\mathbf{1}^{\mathsf{T}}$ and on the right by c, and we find

$$b^{\mathsf{T}}Ac + b^{\mathsf{T}}c^2 = \mathbf{1}^{\mathsf{T}}B^{\mathsf{T}}GBc = b^{\mathsf{T}}\mathbf{1}b^{\mathsf{T}}c = \frac{1}{2}.$$

By evaluating $b^{\mathsf{T}}c^2 - \frac{1}{3}$, it is found that t must be chosen as $t = \frac{1}{2}$ or as one of the four real solutions of the polynomial equation

$$3t^4 - 12t^3 - t^2 + 8t - 1 = 0.$$

For simplicity we will adopt the choice $t = \frac{1}{2}$, and this gives the method

$$\begin{bmatrix} A & U \\ B & V \end{bmatrix} = \left[\begin{array}{cccc|cc} \frac{1}{12} & 0 & 0 & 0 & 1 & \frac{1}{2} \\ -\frac{1}{3} & \frac{1}{6} & 0 & 0 & 1 & 1 \\ \frac{5}{3} & -\frac{2}{3} & \frac{1}{6} & 0 & 1 & -1 \\ \frac{7}{6} & -\frac{5}{12} & \frac{1}{12} & \frac{1}{12} & 1 & -\frac{1}{2} \\ \hline \frac{2}{3} & -\frac{1}{6} & -\frac{1}{6} & \frac{2}{3} & 1 & 0 \\ 1 & -\frac{1}{2} & \frac{1}{2} & -1 & 0 & -1 \end{array}\right].$$

A suitable starting method for this method is found based on the Runge–Kutta method:

$$\begin{array}{c|ccc} 0 & & & \\ \frac{1}{2} & \frac{1}{2} & & \\ 1 & \frac{373}{550} & \frac{177}{550} & \\ 0 & \frac{8233}{50976} & -\frac{30749}{152928} & \frac{3025}{76464} \\ \hline & 0 & -\frac{383}{648} & \frac{275}{1296} \quad 1 \end{array}.$$

If this yields the mapping R_h, then the two components of the starting method are given by

$$S_h y_0 = \begin{bmatrix} y_0 \\ \frac{1}{2}(R_h + R_{-h}) - y_0 \end{bmatrix}. \tag{5.5}$$

This method, which we will denote by 4124, will be used as a representative method for the large family of possible fourth order methods.

5.2. A method with $rs = 34$. An alternative is to choose $r = 3$, as in the thesis [11]; this makes it possible to reduce two of the diagonals of A to zero. We will present a method based on a similar ansatz in which $V = \operatorname{diag}(1, i, -i)$. However, for practical use, we will convert this to real form using the transformation $U \mapsto UT$, $B \mapsto T^{-1}B$, $V \mapsto T^{-1}VT$, where

$$T = \begin{bmatrix} 1 & 0 & 0 \\ 0 & 1 & -i \\ 0 & 1 & i \end{bmatrix}, \quad T^{-1} = \begin{bmatrix} 1 & 0 & 0 \\ 0 & \frac{1}{2} & \frac{1}{2} \\ 0 & \frac{1}{2}i & -\frac{1}{2}i \end{bmatrix}, \quad V = \begin{bmatrix} 1 & 0 & 0 \\ 0 & 0 & 1 \\ 0 & -1 & 0 \end{bmatrix}.$$

In the complex representation of the method, we assume that U, B, and G take the forms

$$U = \begin{bmatrix} \mathbf{1} & u & \overline{u} \end{bmatrix}, \qquad B = \begin{bmatrix} b^{\intercal} \\ \beta^{\intercal} \\ \overline{\beta}^{\intercal} \end{bmatrix}, \quad G = \operatorname{diag}(1, g, g),$$

where $b \in \mathbb{R}^4$ is symmetric and β, $u \in \mathbb{C}^4$ are antisymmetric. Suitable values of these vectors, to ensure that the method is G-symplectic, parasitism free, and has the required order and that $a_{11} = a_{44} = 0$, are

$$b = \begin{bmatrix} -\frac{1}{10} \\ \frac{3}{5} \\ \frac{3}{5} \\ -\frac{1}{10} \end{bmatrix}, \quad \beta = \begin{bmatrix} -\frac{1+i\sqrt{5}}{5} \\ \frac{6}{5} \\ -\frac{6}{5} \\ \frac{1+i\sqrt{5}}{5} \end{bmatrix}, \quad u = \begin{bmatrix} -\frac{\sqrt{5}+i}{24} \\ -\frac{i}{24} \\ \frac{i}{24} \\ \frac{\sqrt{5}+i}{24} \end{bmatrix}, \quad g = -\frac{1}{48}.$$

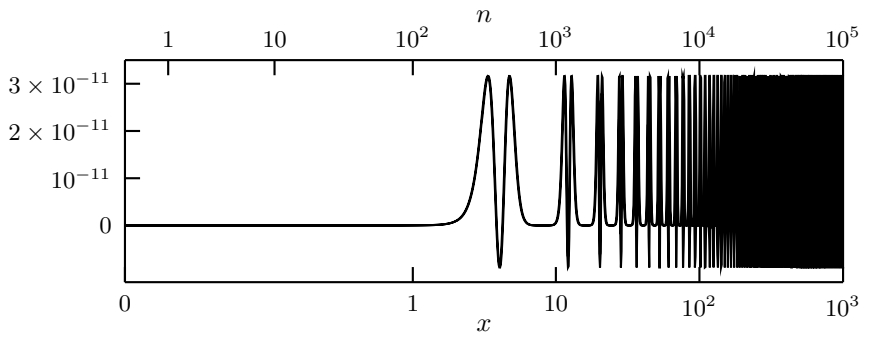

FIG. 13. *The variation in the Hamiltonian for the simple pendulum with initial value* $[0,3]^{\intercal}$ *using the Gauss method with* $h = 0.01$.

The transformed method with real coefficients is given by

$$\begin{bmatrix} A & UT \\ T^{-1}B & T^{-1}VT \end{bmatrix} = \left[\begin{array}{cccc|ccc} 0 & 0 & 0 & 0 & 1 & -\frac{1}{12}\sqrt{5} & -\frac{1}{12} \\ -\frac{1}{12} & \frac{1}{4} & 0 & 0 & 1 & 0 & -\frac{1}{12} \\ -\frac{7}{60} & \frac{7}{10} & \frac{1}{4} & 0 & 1 & 0 & \frac{1}{12} \\ -\frac{1}{5} & \frac{7}{10} & \frac{1}{2} & 0 & 1 & \frac{1}{12}\sqrt{5} & \frac{1}{12} \\ \hline -\frac{1}{10} & \frac{3}{5} & \frac{3}{5} & -\frac{1}{10} & 1 & 0 & 0 \\ -\frac{1}{5} & \frac{6}{5} & -\frac{6}{5} & \frac{1}{5} & 0 & 0 & 1 \\ \frac{1}{5}\sqrt{5} & 0 & 0 & -\frac{1}{5}\sqrt{5} & 0 & -1 & 0 \end{array}\right]. \tag{5.6}$$

This method will be denoted by 4134.

5.3. Comparison with Gauss method. Before proceeding to a range of numerical comparisons, in Figures 13–15 we compare the performance of the new methods, 4124 and 4134, with that of the classical Gauss Runge–Kutta method with order $p = 4$, which is known to be symplectic. In each case the simple pendulum will be used as the test problem with initial value $y = [0,3]^{\intercal}$ and stepsize $h = 0.01$. The Gauss method has the Runge–Kutta tableau:

$$\begin{array}{c|cc} \frac{1}{2} - \frac{\sqrt{3}}{6} & \frac{1}{4} & \frac{1}{4} - \frac{\sqrt{3}}{6} \\ \frac{1}{2} + \frac{\sqrt{3}}{6} & \frac{1}{4} + \frac{\sqrt{3}}{6} & \frac{1}{4} \\ \hline & \frac{1}{2} & \frac{1}{2} \end{array}. \tag{5.7}$$

6. Numerical simulations. This section presents the results of numerical methods constructed in this paper for two types of problems: Hamiltonian problems and problems with quadratic invariants. The aim is to observe the ability of the methods to provide qualitatively correct numerical results over long time.

6.1. The Kepler problem: Variation in the Hamiltonian. The Kepler problem describes the motion of a planet revolving around the sun, which is considered to be fixed at the origin. The equations of motion are defined by the separable Hamiltonian system

$$H = \frac{1}{2}(p_1^2 + p_2^2) - \frac{1}{\sqrt{q_1^2 + q_2^2}},$$

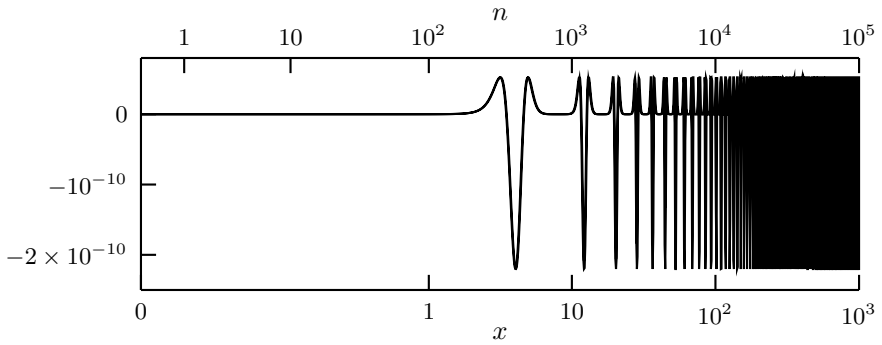

FIG. 14. *The variation in the Hamiltonian for the simple pendulum with initial value* $[0, 3]^\intercal$*, using method* 4124 *with* $h = 0.01$.

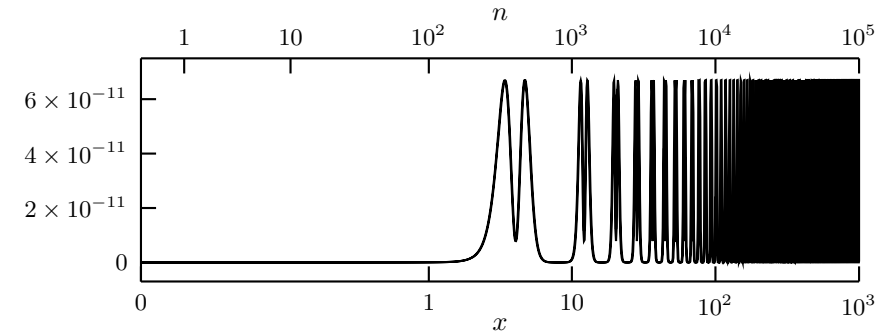

FIG. 15. *The variation in the Hamiltonian for the simple pendulum with initial value* $[0, 3]^\intercal$*, using method* 4134 *with* $h = 0.01$.

where $q = [q_1, q_2]^\intercal$ are the generalized position coordinates of the body and $p = [p_1, p_2]^\intercal$ are the generalized momenta. Writing $y = p \oplus q$, we can write the equations of motion in the form

$$\begin{aligned} y_1' &= \frac{-y_3}{(y_3^2 + y_4^2)^{\frac{3}{2}}}, \\ y_2' &= \frac{-y_4}{(y_3^2 + y_4^2)^{\frac{3}{2}}}, \\ y_3' &= y_1, \\ y_4' &= y_2. \end{aligned}$$

The system has two conserved quantities of interest, namely, the total energy H and the angular momentum L given as

$$L = q_1 p_2 - q_2 p_1 = y_3 y_2 - y_4 y_1.$$

The initial conditions are taken to be

$$[y_1, y_2, y_3, y_4]^\intercal = [p_1, p_2, q_1, q_2]^\intercal = \left[0, \sqrt{\frac{1+e}{1-e}}, 1-e, 0\right]^\intercal,$$

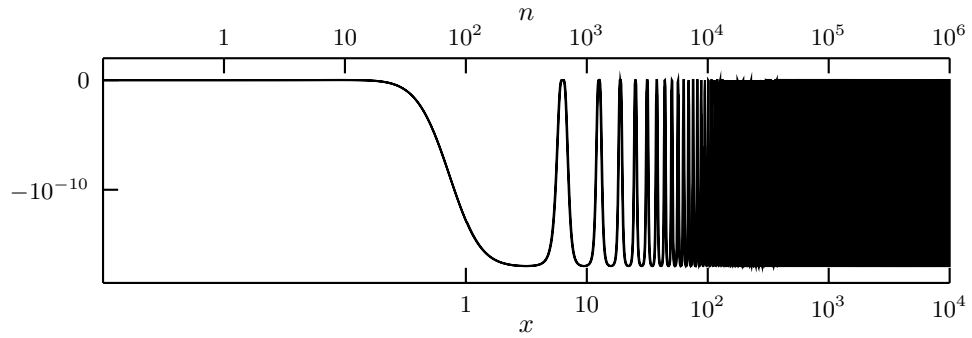

FIG. 16. *The variation in the Hamiltonian for the Kepler problem with* $e = 0.3$*, using Gauss with* $h = 0.01$.

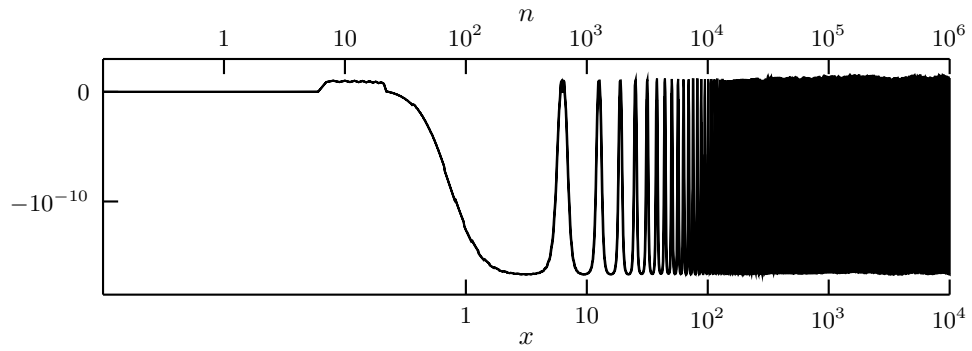

FIG. 17. *The variation in the Hamiltonian for the Kepler problem with* $e = 0.3$*, using* $N^6PN^{14}P$ *with* $h = 0.01$.

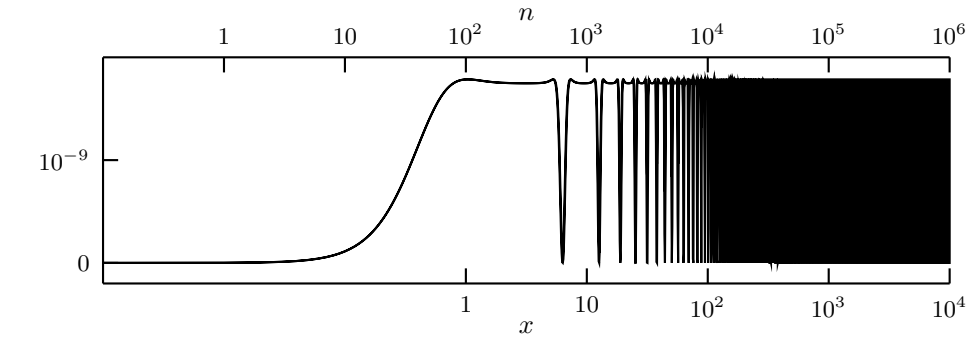

FIG. 18. *The variation in the Hamiltonian for the Kepler problem with* $e = 0.3$*, using* 4124 *with* $h = 0.01$.

where $0 \leq e < 1$ is the eccentricity of the elliptic orbits which are formed by the motion of one body around the other. In the simulations reported here, $e = 0.3$.

In Figures 16–19, we compare the performance of three methods introduced in this paper with a symplectic Runge–Kutta method. The four methods are (a) the two-stage Gauss method, (b) the composition method $N^6PN^{14}P$, (c) a two-input method referred to as 4124, and (d) a three-input method 4134.

6.2. The Kepler problem: Variation in the angular momentum. For this problem, the Gauss method preserves angular momentum exactly, and this should

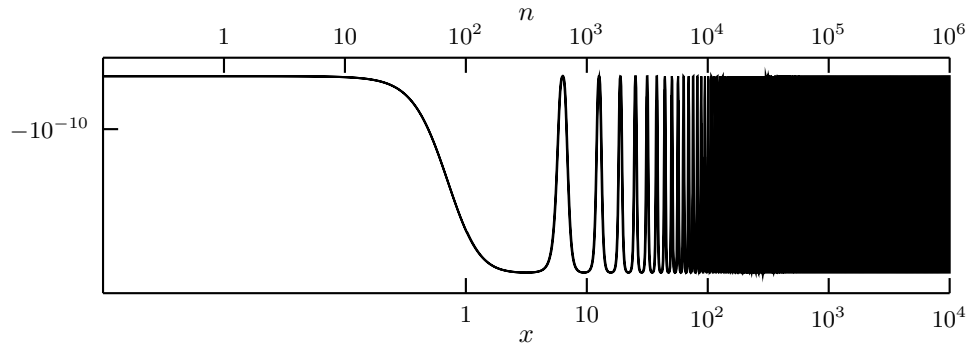

FIG. 19. *The variation in the Hamiltonian for the Kepler problem with* $e = 0.3$*, using* 4134 *with* $h = 0.01$.

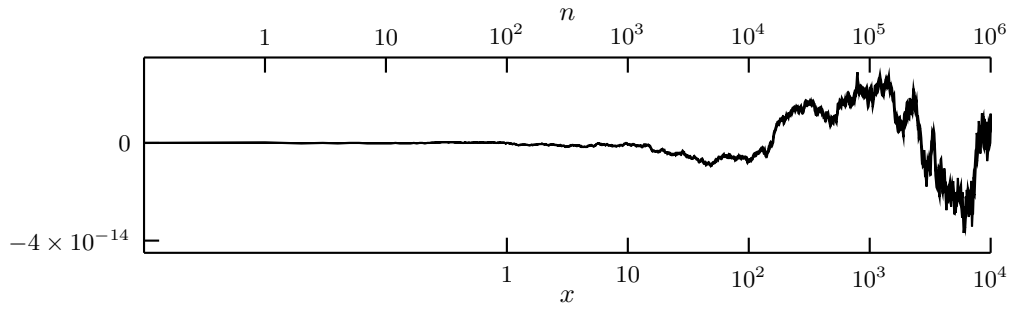

FIG. 20. *Variation of the angular momentum for the Kepler problem with* $e = 0.3$*, using the Gauss method with* $h = 0.01$.

be observed in simulations as shown in Figure 20. Note that no compensation for the accumulation of round-off errors has been used in these computations and the moderate values of the deviation after 10^6 steps should be judged as a verification of this. In Figures 21–23, results are also given for the composition method $N^6PN^{14}P$ and the parasitism-free methods 4124 and 4134.

6.3. Euler equations for rigid body motion: Variation in quadratic invariants. Rigid bodies are solid objects such that the distance between any two points on or inside it is constant. The mathematical equations governing the motion of a rigid body were discovered by Euler and are given as

$$\frac{dy_1}{dx} = \frac{I_2 - I_3}{I_1} y_2 y_3,$$
$$\frac{dy_2}{dx} = \frac{I_3 - I_1}{I_2} y_3 y_1,$$
$$\frac{dy_3}{dx} = \frac{I_1 - I_2}{I_3} y_1 y_2,$$

where y_1, y_2, y_3 are the components of angular velocity about the principal axes and I_1, I_2, I_3 are the principal moments of inertia. The motion of rigid body has the following two underlying quadratic invariants, namely, the kinetic energy H and the squared norm of angular momentum A given as

$$H = \frac{1}{2} y^{\intercal} \operatorname{diag}(I_1, I_2, I_3) y, \tag{6.1}$$

$$A = y^{\intercal} \operatorname{diag}(I_1^2, I_2^2, I_3^2) y. \tag{6.2}$$

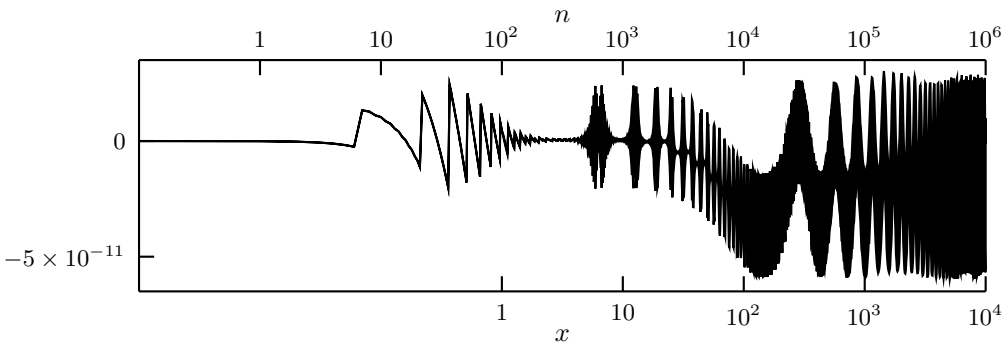

FIG. 21. *The variation in the angular momentum for the Kepler problem with* $e = 0.3$*, using* $N^6PN^{14}P$ *with* $h = 0.01$.

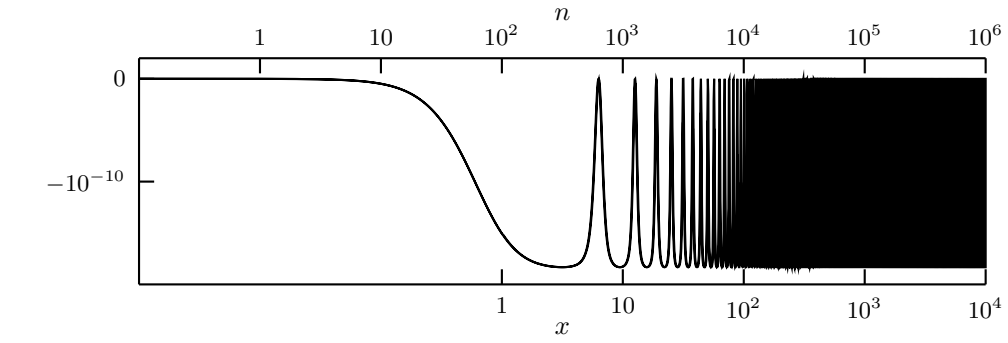

FIG. 22. *The variation in the angular momentum for the Kepler problem with* $e = 0.3$*, using* 4124 *with* $h = 0.01$.

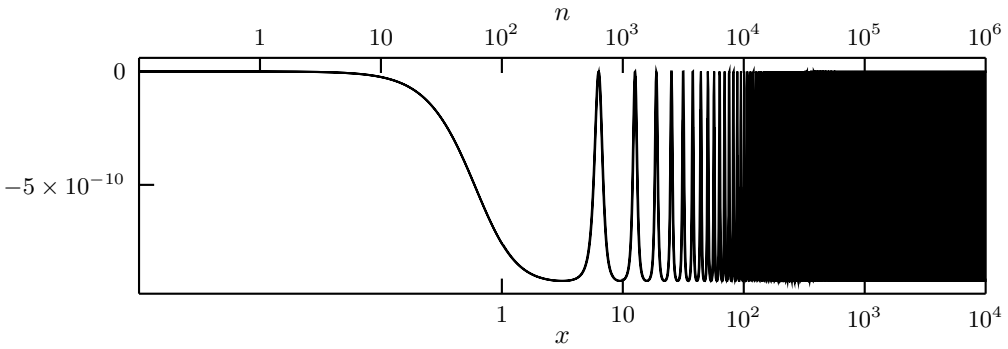

FIG. 23. *The variation in the angular momentum for the Kepler problem with* $e = 0.3$*, using* 4134 *with* $h = 0.01$.

Experiments were performed for the case $I_1 = 5$, $I_2 = 6$, $I_3 = 7$, using initial value $y = [1, 0, 1]^{\mathsf{T}}$. Results for the method 4124 using $h = 0.001$ are presented in Figure 24. Simulations carried out with other methods including N^6P are very similar, and the figure presented should be regarded as being representative. The deviations from the initial value are similar to what would be formed through the growth of round-off errors in the individual steps.

In Figure 25 we give results for a representative G-symplectic method applied to the same problem but where the deviation of A, rather than H is plotted. The results look very similar but scaled up approximately in proportion to $A(0)/H(0)$.

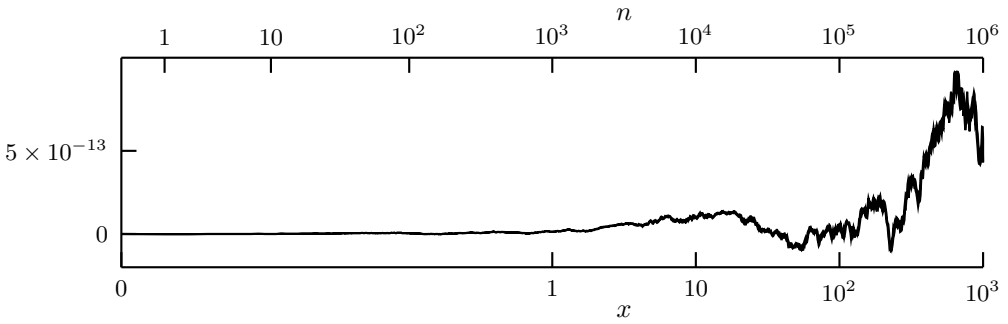

FIG. 24. *Deviation of the energy from its initial value for the Euler rigid body problem with* $h = 0.001$ *using* 4124.

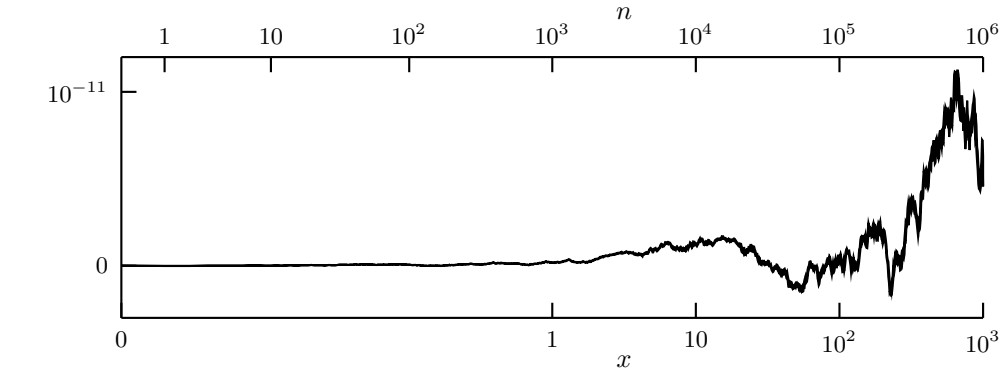

FIG. 25. *Deviation of the squared norm of the angular momentum from its initial value for the Euler rigid body problem with* $h = 0.001$ *using* 4124.

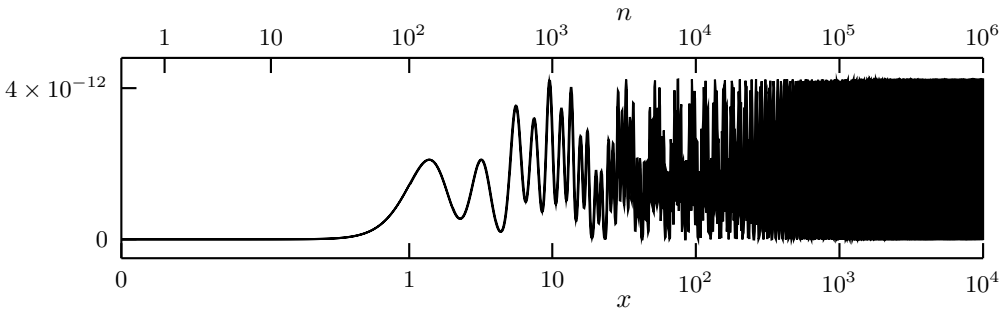

FIG. 26. *The Heńon–Heiles problem solved by the Gauss method with* $h = 0.01$.

6.4. The Heńon–Heiles problem. We now consider simulations based on the Heńon–Heiles problem [16] with a specific initial value

$$\begin{aligned} y_1' &= y_3, & y_1(0) &= 0,\\ y_2' &= y_4, & y_2(0) &= 0,\\ y_3' &= -y_1 - 2y_1y_2, & y_3(0) &= \sqrt{0.3185},\\ y_4' &= -y_2 - y_1^2 + y_2^2, & y_4(0) &= 0. \end{aligned}$$

This problem is based on the Hamiltonian

$$H = \frac{1}{2}(y_3^2 + y_4^2) + \frac{1}{2}(y_1^2 + y_2^2) + y_1^2y_2 - \frac{1}{3}y_2^3.$$

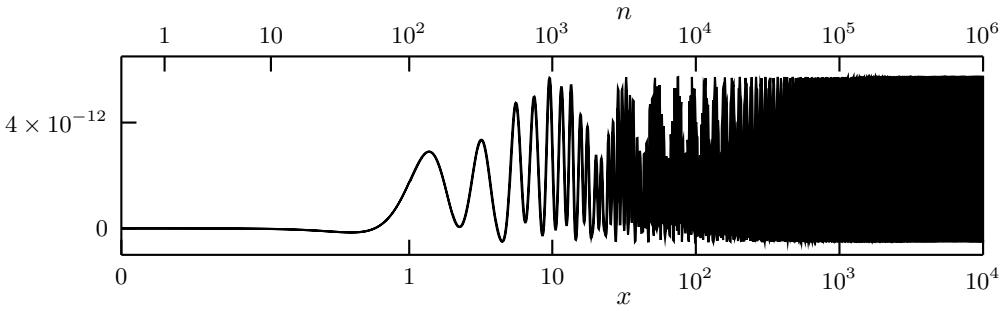

FIG. 27. *The Heńon–Heiles problem solved by the* 4124 *method with* $h = 0.01$.

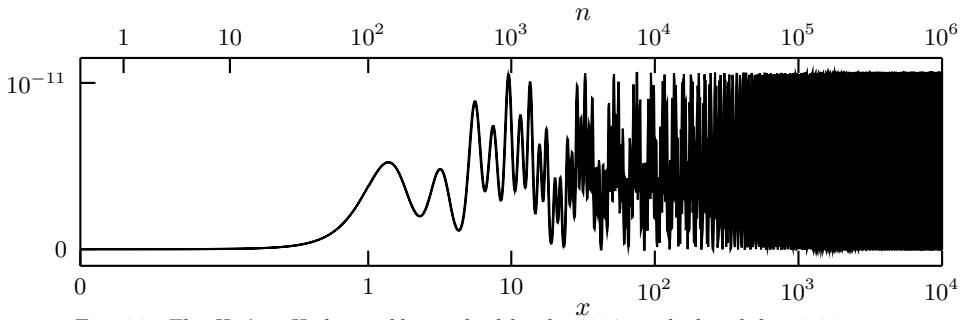

FIG. 28. *The Heńon–Heiles problem solved by the* 4134 *method with* $h = 0.01$.

The deviation of H from its initial value is shown in three simulations: for Gauss in Figure 26, for 4124 in Figure 27, and for 4134 in Figure 28.

Acknowledgments. The authors thank the anonymous referees for their comments, which have led to substantial improvements to this paper. The first author wishes to thank the Marsden Fund of New Zealand for financial support. The second author wishes to thank the National University of Science and Technology (NUST), Pakistan and HEC of Pakistan for financial support during his Ph.D. studies. The third author thanks the London Mathematical Society, the Royal Society of London, and the Marsden fund for making possible a number of visits to Auckland. He also thanks the University of Auckland for hosting these visits. The fourth author acknowledges financial support from EPSRC UK.

REFERENCES

[1] V. I. ARNOLD, *Mathematical Methods for Classical Mechanics*, Springer, New York, 1978.
[2] J. C. BUTCHER, *Diagonally-implicit multi-stage integration methods*, Appl. Numer. Math., 11 (1993), pp. 347–363.
[3] J. C. BUTCHER, *General linear methods*, Acta Numer., 15 (2006), pp. 157–256.
[4] J. C. BUTCHER, *Numerical Methods for Ordinary Differential Equations*, 2nd ed., Wiley, New York, 2008.
[5] J. C. BUTCHER, A. T. HILL, AND T. J. T. NORTON, *Symmetric general linear methods*, in preparation.
[6] J. C. BUTCHER AND Z. JACKIEWICZ, *Diagonally implicit general linear methods for ordinary differential equations*, BIT, 33 (1993), pp. 452–472.
[7] P. CHARTIER, E. FAOU, AND A. MURUA, *An algebraic approach to invariant preserving integrators: The case of quadratic and Hamiltonian invariants*, Numer. Math., 103 (2006), pp. 575–590.

[8] G. Dahlquist, *Convergence and stability in the numerical solution of ordinary differential equations*, Math. Scand., 4 (1956), pp. 33–53.
[9] R. D'Ambrosio, E. Hairer, and C. J. Zbinden, *G-symplecticity implies conjugate symplecticity of the underlying one-step method*, BIT, 53 (2013), pp. 867–872.
[10] T. Eirola and J. M. Sanz-Serna, *Conservation of integrals and symplectic structure in the integration of differential equations by multistep methods*, Numer. Math., 61 (1992), pp. 281–290.
[11] Y. Habib, Long-Term Behaviour of G-Symplectic Methods, Ph.D. thesis, University of Auckland, Auckland, NZ, 2010.
[12] E. Hairer, *Conjugate-symplecticity of linear multistep methods*, J. Comput. Math., 26 (2008), pp. 657–659.
[13] E. Hairer and C. Lubich, *Symmetric multistep methods over long times*, Numer. Math., 97 (2004), pp. 699–723.
[14] E. Hairer, C. Lubich, and G. Wanner, *Geometric Numerical Integration, Structure-Preserving Algorithms for Ordinary Differential Equations*, 1st ed., Springer, New York, 2003.
[15] E. Hairer, C. Lubich, and G. Wanner, *Geometric Numerical Integration, Structure-Preserving Algorithms for Ordinary Differential Equations*, 2nd ed., Springer, New York, 2006.
[16] M. Heńon, M. and C. Heiles, *The applicability of the third integral of motion: Some numerical experiments*, Astron. J., 69 (1964), pp. 73–79.
[17] F. M. Lasagni, *Canonical Runge-Kutta methods*, ZAMP, 30 (1988), pp. 952-953.
[18] R. I. McLachlan, *On the numerical integration of ordinary differential equations by symmetric composition methods*, SIAM J. Sci. Comput., 16 (1995), pp. 151–168.
[19] G. D. Quinlan and S. Tremaine, *Symmetric multistep methods for the numerical integration of planetary orbits*, Astron. J., 100 (1990), pp. 1694–1700.
[20] J. M. Sanz-Serna, *Runge–Kutta schemes for Hamiltonian systems*, BIT, 28 (1988), pp. 877–883.
[21] J. M. Sanz-Serna, *Symplectic integrators for Hamiltonian problems*, Acta Numer., 1 (1992), pp. 243–286.
[22] J. M. Sanz-Serna and L. Abia, *Order conditions for canonical Runge–Kutta schemes*, SIAM J. Numer. Anal., 28 (1991), pp. 1081–1096.
[23] J. M. Sanz-Serna and M. P. Calvo, *Numerical Hamiltonian Problems*, 1st ed., Chapman and Hall, London, 1994.
[24] Y. B. Suris, *On the conservation of symplectic structure in the numerical solution of Hamiltonian systems*, in Numerical Solution of Ordinary Differential Equations, ed., S. S. Fillipov, Keldysh Institute of Applied Mathematics, USSR Academy of Sciences, Moscow, 1988, pp. 148–160.
[25] M. Suzuki, *Fractal decomposition of exponential operators with applications to many-body theories and Monte Carlo simulations*, Phys. Lett. A, 146 (1990), pp. 319–323.
[26] L. Verlet, *Computer "experiments" on classical fluids.* I. *Thermodynamical properties of Lennard–Jones molecules*, Phys. Rev., 159 (1967), pp. 98–103.
[27] H. Yoshida, *Construction of higher order symplectic integrators*, Phys. Lett. A, 150 (1990), pp. 262–268.